

# Using Synthetic Biology to Engineer Spatial Patterns

Javier Santos-Moreno\* and Yolanda Schaerli\*

Synthetic biology has emerged as a multidisciplinary field that provides new tools and approaches to address longstanding problems in biology. It integrates knowledge from biology, engineering, mathematics, and biophysics to build—rather than to simply observe and perturb—biological systems that emulate natural counterparts or display novel properties. The interface between synthetic and developmental biology has greatly benefitted both fields and allowed to address questions that would remain challenging with classical approaches due to the intrinsic complexity and essentiality of developmental processes. This Progress Report provides an overview of how synthetic biology can help to understand a process that is crucial for the development of multicellular organisms: pattern formation. It reviews the major mechanisms of genetically encoded synthetic systems that have been engineered to establish spatial patterns at the population level. Limitations, challenges, applications, and potential opportunities of synthetic pattern formation are also discussed.

## 1. Introduction

Synthetic biology is a rising interdisciplinary field that adopts and applies concepts from engineering, such as modelling, modularity, and part standardization to construct novel biological systems.<sup>[1–3]</sup> These systems have the potential to lead to important clinical and industrial applications, for example, by providing novel approaches to detect and treat diseases and to produce fine chemicals, biofuels, and smart materials.<sup>[4–7]</sup> Another major power of synthetic biology is that it allows us to construct simplified versions of complex natural systems that are amenable to study, thus permitting researchers to infer general underlying principles and to build knowledge in a bottom-up manner. When building a synthetic system inspired by a natural counterpart, researchers have the freedom to focus on the elements of interest, while avoiding confounding factors. This provides a complementary approach to study the mechanism, organization, function, and evolution of natural biological systems and processes.

Here, we review how synthetic biology can help to understand pattern formation, which is a crucial process during the

development of multicellular organisms. Embryonic development often consists of three major phases—patterning, differentiation, and morphogenesis—that generally take place in a sequential manner. First a pattern is established by an (non-random) arrangement of gene expression, then cells commit (differentiate) to a given state, and finally a particular physical form is created (morphogenesis). Thus, it all starts with patterning—the development of differential characteristics within a group of cells that were initially genetically and phenotypically homogeneous. Understanding the networks, mechanisms, and cues underlying biological pattern formation is one of the main challenges of developmental biology.

Synthetic biology offers researchers a novel approach to tackle this challenge. As highlighted by Jamie Davies in his excel-


lent review,<sup>[8]</sup> a synthetic biology approach applied to developmental research allows us to test and discover basic, general principles underlying complex embryogenesis processes. Classical developmental biology is of course still needed to elucidate the mechanistic details of any given natural developing system, but synthetic biology offers unprecedented tools to address the same problem from a different angle, allowing us to generalize specific discoveries into broad concepts and ideas. Even more, the construction of synthetic developmental systems allows for the study of “roads not taken” by evolution, i.e., solutions that are not found in natural systems. The comparison of different solutions for the same problem can be highly informative in terms of selection pressures, adaptation, and evolutionary constraints.

In this Progress Report, we provide an overview of recently developed synthetic patterning systems and show the varied solutions and approaches that researchers have applied to achieve particular spatial arrangements. We focus on patterning at the population level driven by genetically encoded synthetic systems, obviating organization at other scales such as intracellular patterning<sup>[9]</sup> and technology-based “external” patterning platforms such as inkjet printing.<sup>[10,11]</sup> We also do not cover patterns generated with DNA or proteins only,<sup>[12,13]</sup> but concentrate our discussion mainly on cell-based patterns with the addition of few patterns generated in cell-free expression systems.

We begin with Lewis Wolpert’s “positional information” patterning and in particular with the stripe pattern—the spatial pattern most extensively studied by synthetic biologists. We then discuss patterning systems based on phase separation, lateral inhibition, and mechanical forces, before highlighting

Dr. J. Santos-Moreno, Prof. Y. Schaerli  
Department of Fundamental Microbiology  
University of Lausanne  
Biophore Building  
1015 Lausanne, Switzerland

E-mail: javier.santosmoreno@unil.ch; yolanda.schaerli@unil.ch

 The ORCID identification number(s) for the author(s) of this article can be found under <https://doi.org/10.1002/adbi.201800280>.

DOI: 10.1002/adbi.201800280

the efforts made toward building synthetic “reaction–diffusion” Turing patterns. Next, we cover spatial patterns induced by temporal oscillations and those that are controlled by light. Finally, we close by highlighting the challenges and opportunities of the field, including potential applications of synthetic patterning systems.

## 2. The French Flag Model: Patterning in Response to a Concentration Gradient

Patterning events in embryos are frequently controlled by morphogens, which are molecular species, most commonly secreted, that determine cell fate in a concentration-dependent and/or time-dependent manner.<sup>[14–17]</sup> The French flag model<sup>[18]</sup> (Figure 1A) illustrates how the concentration of the morphogen can provide positional information that is interpreted across a field of cells to trigger different gene expression programs (“blue,” “white,” or “red” programs) depending on the position of each cell within the gradient. A common pattern in response to a morphogen gradient is the stripe pattern (also called band-pass filter), in which expression of a specific gene is only triggered at intermediate concentrations of the morphogen, but not at low and high morphogen concentrations (Figure 1B). The question of how gene regulatory networks produce such stripes in a morphogen gradient is a pivotal one in developmental biology. Several computational studies addressed this question and identified gene regulatory networks (GRNs) capable of stripe formation.<sup>[19–22]</sup> Moreover, stripe patterns have been successfully recreated in synthetic systems (Figure 1C).

Among the simplest stripe-forming networks identified are the four incoherent feed-forward loop (IFFL) topologies, (Figure 2A(I1–I4)),<sup>[23]</sup> composed of 3 nodes. We define a node as an interaction unit of a GRN where input signal(s) are received, and subsequent output signal(s) are generated; thus, a node can correspond to a single or multiple gene(s) (see for example subpanel I2 in Figure 2C). In feed-forward loops, the morphogen-detecting node (N1) directly regulates the stripe-producing node (N3), but these two nodes are also connected indirectly through an intermediate node (N2). A feed-forward loop is considered to be incoherent when the net signs of the two regulation paths (the direct and the indirect paths) are opposite, i.e., one is activating and one is repressing.<sup>[23]</sup>

Indeed, most of the synthetic stripe-forming circuits built so far are using one of the four IFFL topologies (Table 1). Here, we will describe them one by one in more detail.

### 2.1. Stripe-Forming Synthetic GRNs with I1 Topology

All stripe-forming IFFLs operate with the same underlying logic: at low morphogen (input) concentrations the output is OFF, but as morphogen levels increase the output is activated (ON) and further brought down again (OFF) at high morphogen levels. Nevertheless, the specific molecular implementation of that logic varies depending on the IFFL topology. For instance, in the I1 topology the output node (N3) is not expressed at low morphogen concentration due to a lack of activation. At intermediate morphogen concentrations it is highly expressed due



**Javier Santos-Moreno** is a postdoctoral researcher in the Schaerli laboratory at the Department of Fundamental Microbiology, University of Lausanne, Switzerland. Following MSc studies at the University of Salamanca, Spain, and at the University Pompeu Fabra, Spain, he moved to Paris, France, for his PhD, in which he studied

protein secretion in bacteria under the supervision of Olivera Francetic at the Pasteur Institute and Guy Tran Van Nhieu at Collège de France. In the group of Prof. Schaerli, he designs and constructs synthetic gene regulatory networks for patterning.



**Yolanda Schaerli** is an assistant professor of synthetic biology at the Department of Fundamental Microbiology, University of Lausanne, Switzerland. Her previous positions were at the University of Zurich (junior group leader), the Centre for Genomic Regulation, Barcelona (postdoc), and the University of Cambridge

(PhD). Research in her laboratory uses a bottom-up synthetic biology approach to understand the mechanisms, properties, and evolution of gene regulatory networks, especially those involved in pattern formation.

to the activation by the morphogen receiving node (N1), and at high morphogen concentration it is repressed by the intermediate node (N2) that itself is activated by N1 (Figure 2A,B).

The first synthetic stripe-forming GRNs with an I1 topology were built by Entus et al.<sup>[24]</sup> The circuits were implemented in *Escherichia coli* (*E. coli*), and formed a green fluorescent protein (GFP) stripe in a gradient of isopropyl  $\beta$ -D-1-thiogalactopyranoside (IPTG). The circuit depicted in Figure 2C relies on protein:DNA interactions, namely transcription factor or RNA polymerase binding to operator and promoter regions, respectively. As a proof that other molecular interactions also enable band-pass filter construction, two other variants were built in which the repression interaction was achieved through RNA:RNA and protein:protein interactions.

Few years later, Schaerli et al. also implemented an I1 topology in a study that explored the design space of 3-node stripe-forming networks. In fact, the authors built all four IFFL network topologies, demonstrated their stripe-forming capabilities and characterized them in detail.<sup>[19]</sup> The four GRNs were constructed in *E. coli* using viral RNA polymerases as activators and bacterial transcription factor-driven repression.

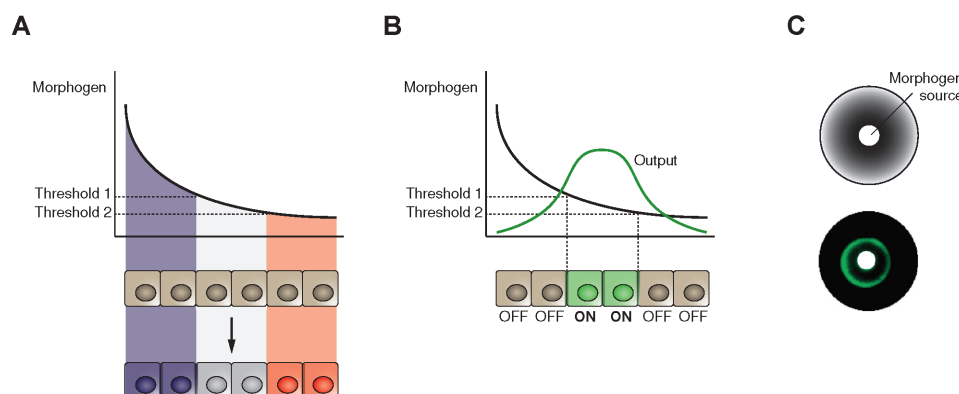


**Figure 1.** The French flag model of pattern formation in response to a morphogen gradient. A) A population of cells that is initially undifferentiated responds to different concentrations of a morphogen by activating “blue,” “white,” and “red” genetic programs. B) Interpretation of a morphogen gradient as a stripe pattern. Only cells subjected to intermediate morphogen levels produce a positive response (e.g., green fluorescence), resulting in an off–ON–off (or low–HIGH–low) spatial pattern. C) Example of stripe formation by a synthetic GRN. A paper disc in the center of an agar plate releases the morphogen by diffusion, creating a circular gradient (top, representation). Engineered *E. coli* growing on such an agar plate produce GFP only at intermediate morphogen concentrations, resulting in a ring of green fluorescence (bottom, image). Reproduced with permission.<sup>[19]</sup> Copyright 2014, Macmillan Publishers Limited.

Importantly, controls were performed to discard stripe-like patterns due to metabolic load, i.e., resource limitation for host cell metabolism due to (over)expression of heterologous genes.<sup>[25–27]</sup> While the expression of an heterologous gene under the control of an inducible promoter will normally increase in a monotonic manner with increasing amounts of the inducer, high levels of expression may overwhelm the host’s capacity, resulting in a lower expression of the gene of interest at high inducer levels than at intermediate inducer concentrations—that is, a stripe pattern. Therefore, it is of great importance that supposedly stripe-forming circuits are controlled for metabolic load, since even networks theoretically lacking stripe-forming ability can lead to stripe-like patterns if gene expression poses an excessive burden on cell’s capacity.

## 2.2. The “Favorite” I2 Topology

Most synthetic stripe-forming circuits designed so far rely on an I2 topology. This topology has the particularity of lacking activation reactions—the computing is fully achieved through repression interactions (Figure 2A). Briefly, the output node (N3) is subjected to a double repression both at low and at high morphogen concentrations, which leaves an “open window” for N3 expression only at intermediate levels of the morphogen (Figure 2B). The logic behind N3 expression can be conceptualized as a NOR-gate, which means that the output will only exist when neither of the inputs of nodes 1 and 2 are present.

The first synthetic circuit capable of displaying a stripe pattern in a population of cells was built by Basu et al. in 2005 and it was indeed based on an I2 topology.<sup>[28]</sup> They made use of the *Vibrio fischeri* quorum sensing system to elicit patterning of engineered *E. coli* in response to a chemical concentration gradient. A localized source of “sender” cells produces an acyl-homoserine lactone (AHL) signal that diffuses across an agar plate and functions as a morphogen analogue. Homogeneously distributed “receiver” cells interpret the AHL gradient to form

a low–HIGH–low pattern of a fluorescent reporter (Figure 2C). By modifying the responsiveness of the receiver circuit, authors constructed strains that produce stripes at different AHL concentrations. Further stripe-forming I2 networks were implemented in *E. coli*<sup>[19]</sup> and *Saccharomyces cerevisiae*<sup>[32]</sup> using the same set of repressors, suggesting that some circuit parts may be transferrable to an eukaryotic context after a rapid prototyping in a prokaryotic background.

The few synthetic stripes achieved in a mammalian system rely on I2 and I3 networks.<sup>[35,38,39]</sup> The work by Kämpf et al. demonstrates that mammalian cells also offer a versatile framework to construct, tune, and rewire complex patterning networks.<sup>[38]</sup> To achieve a stripe pattern, not only inducible gene expression but also inducible protein modification and degradation were employed. Connecting multiple stripe-forming networks together and exposing them to two morphogen gradients resulted in new spatial patterns, such as a cross pattern.

## 2.3. Networks Operating with an I3 Topology

In the I3 topology, the input node (N1) activates the intermediate node (N2), which in turn activates the output node (N3). The output node is also directly repressed by the input node. Therefore, the maximum output expression occurs at medium morphogen concentration where there is already activation from node 2, but not yet a high level of repression from node 1 (Figure 2A,B). Stripes based on the I3 topology have been built both in prokaryotic<sup>[19,33,34]</sup> and eukaryotic systems.<sup>[38,39]</sup> Among the bacterial I3 networks, the circuit built by Sohka et al. employed growth inhibition to attain stripe formation: the morphogen analogue is an antibiotic (antibiotic 1) and the output node codes for a resistance gene for a second antibiotic present in the medium (antibiotic 2). Consequently, low concentrations of the morphogen (antibiotic 1) do not activate output gene expression required for cell survival in the presence of antibiotic 2, while high levels of the morphogen (antibiotic 1)

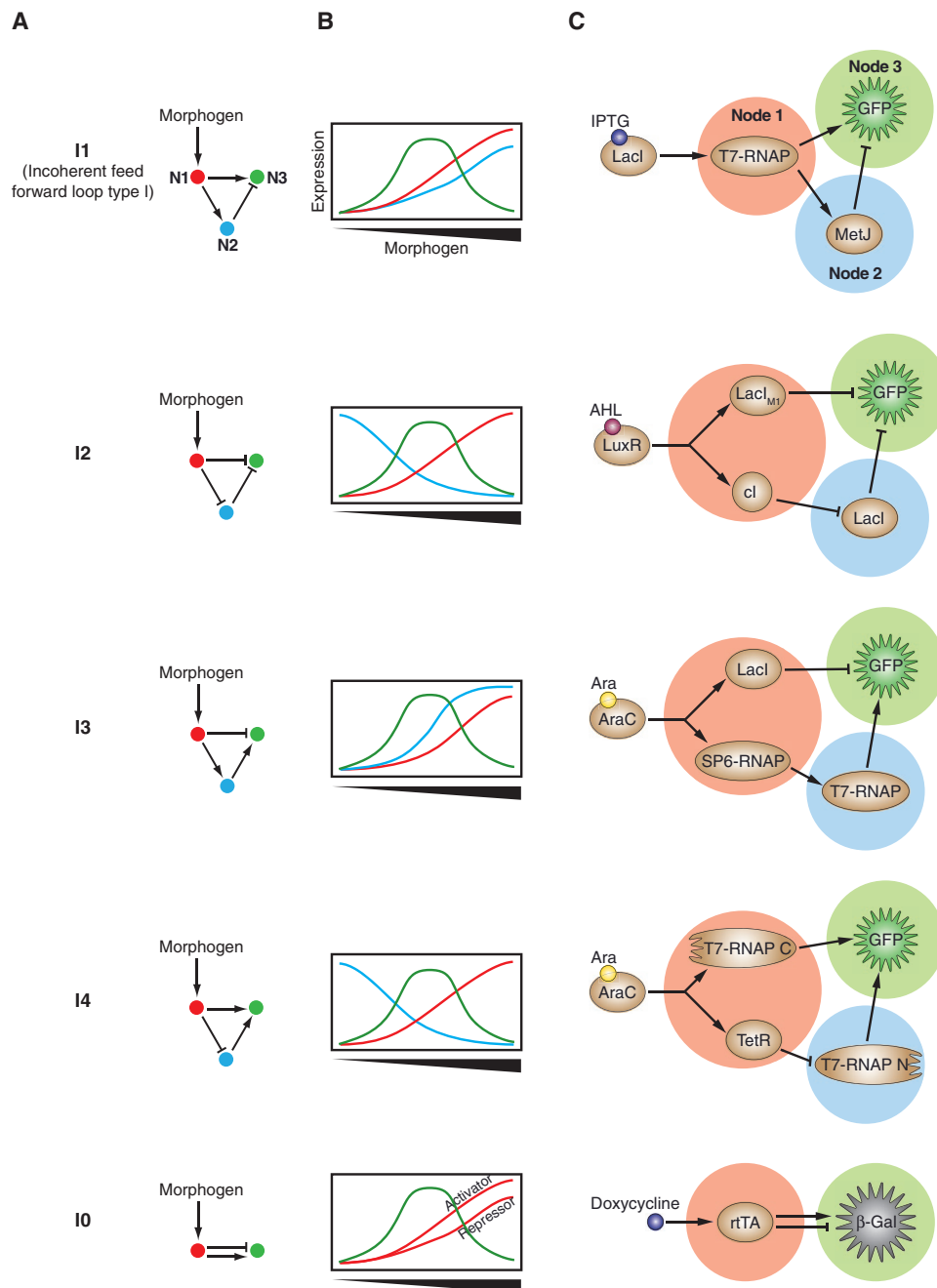


**Figure 2.** Synthetic stripe-forming incoherent feed-forward loops (IFFLs). A) Network topologies of the four 3-node IFFLs (I1–I4) and the minimal 2-node topology I0. Node 1 (N1, red) receives the input morphogen signal, node 2 (N2, blue) provides intermediate regulation, and node 3 (N3, green) forms a stripe in a morphogen gradient, i.e., provides the circuit output. Pointed arrows indicate activation and blunt-end arrows denote repression. B) Gene expression levels of each node (color-coded as in panel A) depicted as a function of morphogen concentration. Reproduced with permission.<sup>[19]</sup> Copyright 2014, Macmillan Publishers Limited. C) Schematic representation of examples of synthetic stripe-forming circuits operating with the corresponding IFFL topologies. In the I1 network by Entus et al. activation relies on the RNA polymerase of the T7 bacteriophage (T7-RNAP), while repression is driven by the transcriptional repressor MetJ. IPTG was used as a morphogen analogue, which induces expression of T7-RNAP from the *lac* promoter.<sup>[24]</sup> The I2 circuit by Basu et al. responds to an AHL gradient produced by a localized source of sender cells. The AHL-bound transcriptional activator LuxR activates the repression-only circuit, which relies on the lambda bacteriophage *cl* repressor, and two versions of the LacI repressor: the wild-type (LacI) and a mutant (LacI<sub>M1</sub>) with a reduced activity.<sup>[28]</sup> The I3 and I4 networks built by Schaefer et al. respond to a gradient of arabinose through the transcriptional regulator AraC of the *ara* operon.<sup>[19]</sup> The I3 network uses two viral RNA polymerases for activation (SP6-RNAP and T7-RNAP) and LacI for repression, whereas the I4 circuit relies on TetR repression and an AND gate implemented through a split T7 polymerase (T7 RNAP-N and T7 RNAP-C).<sup>[29]</sup> In the I0 network built by Buetti-Dinh et al. the doxycycline-induced transcription factor rTA displays both activator and repressor activities, leading to a stripe expression pattern of the downstream  $\beta$ -galactosidase ( $\beta$ -Gal).<sup>[30]</sup>

**Table 1.** Synthetic stripe-forming systems discussed here, in chronological order.

Host system	Topology	Comments	Reference
Cell-free	Simplified <i>Drosophila</i> gap gene system, including I2		[31]
<i>E. coli</i>	I2		[28]
<i>E. coli</i>	I1		[24]
<i>S. cerevisiae</i>	I2		[32]
<i>E. coli</i>	I3		[33]
<i>E. coli</i>	I3		[34]
<i>S. cerevisiae</i>	I0		[30]
Mammalian (CHO derivative)	I2		[35]
<i>E. coli</i>	I0		[36]
<i>E. coli</i>	I4		[37]
Mammalian (HEK-293T)	I2, I3		[38]
<i>E. coli</i>	I0, I1, I2, I3, I4		[19]
<i>E. coli</i>	I4		[29]
Mammalian (hIPSC and hMSC derivative)	I3		[39]
<i>E. coli</i>	I4		[40]
<i>E. coli</i>	Density-dependent motility arrest in an expanding population	Self-organizing	[41]
<i>E. coli</i>	Combination of direct self-activation and indirect negative feedback	Self-organizing	[42]
<i>E. coli</i>	Derived from Payne et al. 2013 <sup>[42]</sup>	Self-organizing	[43]
<i>E. coli</i>	Derived from Payne et al. 2013 <sup>[42]</sup>	Self-organizing	[44]
<i>E. coli</i>	AND gate with two opposing morphogens		[45]

are deleterious for the cells. Hence, cells are only able to grow at intermediate levels of the morphogen.<sup>[33,34]</sup> Moreover, one of the promoters is controllable by IPTG allowing external tunability of the stripe position within the morphogen gradient. The placement of multiple sources of the two antibiotics and IPTG allowed the authors to create complicated, custom-designed patterns.<sup>[33,34]</sup>

#### 2.4. AND-Logic Mediated Expression: The I4 Topology

The I4 topology has the particularity that the stripe-forming node (N3) integrates two activation interactions with an AND-gate logic, which means that N3 only produces an output when both inputs coincide in time and space, but not if only one of them is present. An obvious way to achieve an AND-logic is through the reconstitution of a full-length protein from its constituent split fragments. The split element can either be the regulator that controls expression of the stripe-forming reporter gene (Figure 2C),<sup>[19,29]</sup> or the reporter itself.<sup>[37]</sup> Another handy approach to obtain an AND-gate is through cell growth inhibition: a reporter gene under the control of a concentration-dependent toxic inducer will only be expressed when inducer

concentration is sufficiently high and cells are alive (i.e., the concentration of inducer is not high enough to trigger cell death)—the result is a stripe pattern of the reporter.<sup>[40]</sup>

Instead of using an I4-type incoherent feed-forward loop, an AND-based stripe pattern can be achieved more simply using two opposing morphogen gradients that induce expression of the two halves of a split protein: only when the levels of morphogen 1 and morphogen 2 are sufficiently high are both halves coexpressed.<sup>[45]</sup> However, in this last case, the information gain provided by the synthetic network is lower compared to the I4 network, since a richer input is needed (two opposing morphogen gradients versus a single gradient in I4) to achieve the same output (a stripe).

#### 2.5. A Step Further toward Simplification: The Minimal I0 Topology

The four IFFL topologies discussed above share a common feature: the presence of two pathways (an activating and a repressing one) connecting the input node of the network (N1) to the output node (N3). As discussed already, one of the pathways is direct while the other acts through an intermediate node (N2) that adds an additional layer of regulation and helps position the repression and activation thresholds in the correct order. However, in principle no intermediate node is necessary if the input node acts as a dual regulator capable of both activating and repressing the output node directly (Figure 2).<sup>[15]</sup> Schaeferli et al. termed this minimal stripe-forming network I0.<sup>[19]</sup>

Several studies have indeed managed to minimize stripe-forming GRNs down to an I0 topology.<sup>[19,30,36]</sup> Muranaka and Yokobayashi built an I0 network using riboswitches, which are regulatory elements in the 5′ untranslated region of mRNAs that change structure upon metabolite binding and consequently regulate the expression of the downstream coding sequence.<sup>[46]</sup> The tandem arrangement of an activating and a repressing riboswitch upstream of the coding sequence of GFP resulted in a band-pass response. Importantly, the riboswitches conferring the band-pass behavior were contained within ~300 nucleotides upstream of the reporter, which makes this construct the most compact stripe-forming system built so far.<sup>[36]</sup> Another I0 topology based on transcriptional regulation was implemented in the yeast *S. cerevisiae*.<sup>[30]</sup> A transcription factor acted as activator when bound upstream of the promoter TATA box but also as repressor when bound downstream, leading to a stripe expression pattern of the downstream gene. Schaeferli et al. also engineered such a 2-node synthetic network, and they further modified it to achieve an “anti-stripe” pattern: by increasing the activity of the repressor, its dose-response curve shifted to lower morphogen concentrations than that of the activator; given a basal expression of the activator, the final output was a HIGH–low–HIGH pattern.<sup>[19]</sup>

#### 2.6. Cell-Free Stripe Patterns

Although most of the patterns produced by synthetic biologists are using cells as hosts, few studies also employ cell-free expression systems. One example is the work by Isalan et al.



They developed an in vitro patterning system that roughly emulated early patterning steps of the *Drosophila* embryo.<sup>[31]</sup> The setup consisted of a set of plastic chambers containing a transcription–translation mixture and beads coated with custom DNA sequences. These sequences, encoding repressors and activators, were delivered to the chambers in a homogeneous or gradient distribution. In spite of using a simplified network based on fundamentally different components operating in a radically distinct environment, this in vitro synthetic system succeeded to crudely reconstruct some of the patterns that arise during early fruit fly embryo development. The simplicity of the experimental setup allowed the authors to modify the circuit (e.g., implementing protein degradation or mutually repressive interactions) and characterize the emerging properties.

### 3. Stripe Patterns Independent of Morphogen Gradients

Most synthetic stripe-forming designs use a morphogen gradient as an initial cue to trigger the desired patterning, i.e., they can be roughly categorized as French flag model-based systems. The field of synthetic patterning benefits from designs capable of “reading” and transforming external cues into bespoke configurations, but the ability to form patterns de novo (without any external signal) is also desirable.

The You laboratory has developed a synthetic network that makes bacterial colonies produce a ring pattern without any pre-existing signal.<sup>[42]</sup> Their system combines a direct positive feedback loop with a delayed negative feedback, which depends on the metabolic burden induced by the synthetic network. The result is an mCherry ring at the colony edge, but not only: the pattern also develops in the z-direction, giving an mCherry “dome” structure at the most elevated surface of the microcolony.

This study is an excellent example of how a synthetic system conceived as a proof-of-concept can be further developed and applied to address fundamental biological questions as well as to provide practical and innovative solutions. The network described above was used as a basis to study space-sensing and scale invariance,<sup>[43]</sup> but also to construct bacterial pressure sensors.<sup>[44]</sup> To build these sensors the *csgA* gene from the bacterial curli system, which forms extracellular amyloid fibers, was wired to the patterning network, resulting in a colony with a dome structure of extracellular fibrils to which gold particles were selectively attached.<sup>[44]</sup> When two of such colonies facing each other are sufficiently close, the gold-tagged domes transmit an electrical current. Even more, a higher pressure over the two colonies against each other results in a higher compression of the domes and a concomitant increase in particle–particle contacts, leading to a rise in electrical conductivity—in other words, engineered colonies are capable of sensing pressure.

### 4. Phase Separation: Patterning Driven by Adhesion Properties

Two cell lines with different adhesion properties separate from each other, in a process that is analogous to water and

oil separation into different phases (Figure 3A).<sup>[47,48]</sup> This patterning mechanism plays a role in cell sorting and tissue boundary formation during embryonic development.<sup>[49]</sup> Two main outcomes can be expected from a phase separation: a complete segregation, if the sorting is unconstrained, or a complex, unpredictable pattern of patches of the different phases if the separation is constrained (e.g., by limited physical space or by restricted movement)—analogous to a shallow puddle in which oil forms random patches in water due to limited space in the z-direction. Adhesion-driven sorting is fully determined by physical interactions between cells, but separation depends on some level of cell mobility.

Synthetic phase separation-based systems developed so far in mammalian cells have been implemented by coopting cadherins’ ability to drive cell–cell adhesion. Importantly, not only different types of cadherins but also different levels of surface cadherins of the same type can determine adhesiveness and thus lead to separation (Figure 3B).<sup>[48,50]</sup> Cachat et al. used cadherin-based sorting to achieve incomplete (constrained) separation that resulted in random reticular patterns in 2D and 3D (Figure 3C).<sup>[51,52]</sup> Toda et al. also engineered complex self-organizing 3D patterns using phase separation and lateral inhibition, as we discuss below.<sup>[50]</sup> In bacteria, a recent work employed surface-displayed nanobody–antigen pairs as adhesin analogues to separate cells in different phases depending on their binding capabilities.<sup>[53]</sup>

### 5. Lateral Inhibition: Prevent Your Neighbors of Doing the Same as You

Another way to create patterns is through lateral inhibition. Here, a cell with a particular fate prevents its immediate neighboring cells to adopt the same fate.<sup>[54]</sup> The ligand Delta and the receptor Notch are the best known mediators of lateral inhibition occurring in animal development, for example, for the decision between a neuron or a non-neuron fate in vertebrates.<sup>[55]</sup> Activation of the Notch receptor by its ligand Delta presented on the surface of adjacent cells leads to repression of Delta transcription. Thus, expression of Delta in one cell represses its transcription in the neighboring cells.

Cell fate decision through lateral inhibition has also been reconstructed and studied with the tools of synthetic biology in mammalian cells that do not have a native lateral inhibition mechanism (Figure 4).<sup>[56]</sup> A synthetic circuit built by Matsuda et al. is based on the Delta–Notch interaction and leads to spontaneous bifurcation of a homogenous population into patches of Delta-positive and Delta-negative cells.

A recent seminal publication combined phase separation, programmed cell–cell signaling and lateral inhibition mechanisms to generate multilayered 3D structures reminiscent of those occurring during early embryonic development.<sup>[50]</sup> Custom signaling relied on synNotch receptors, a handy synthetic chimera in which the transmembrane core of Notch receptors (responsible for the self-cleavage that releases the intracellular domain upon ligand binding) can be fused to any desired extracellular (recognition) and intracellular (effector) domains.<sup>[57]</sup> The sorting of two cell populations through cadherin adhesion was combined with synNotch signaling at the

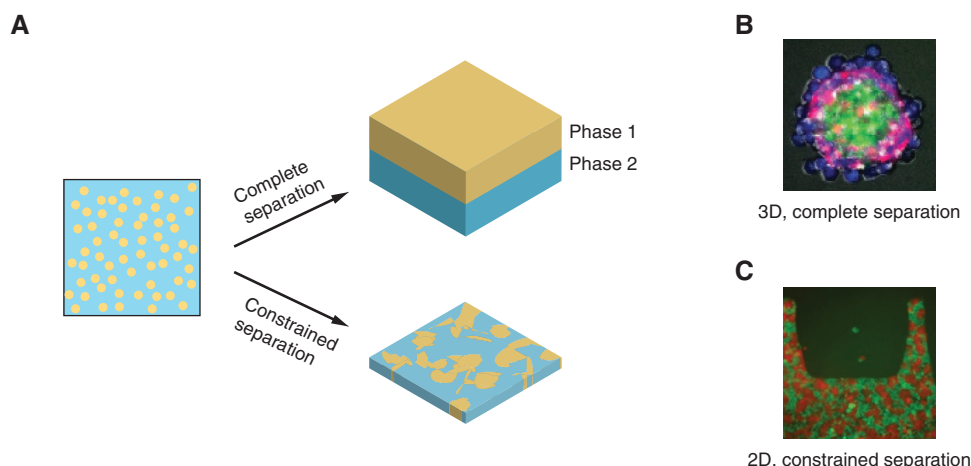


**Figure 3.** Phase separation-driven patterning. A) The differential adhesion of two cell lines determines their separation into two phases. Complete separation occurs when the process is unconstrained; if separation is constrained, e.g. by limited space, the sorting will be incomplete, creating random patches of the two phases. B) Complete self-sorting of cells into a three-layered spherical structure. Mammalian cells were engineered with synthetic circuits for programmed differentiation and cadherin-driven self-organization based on differential adhesion. Reproduced with permission.<sup>[50]</sup> Copyright 2018, American Association for the Advancement of Science (AAAS). C) 2D self-sorting of two mammalian cell lines displaying different surface cadherins. Separation is constrained in the z-direction due to cells' interaction with an adhesive surface; constrained sorting results in a random pattern of patches of the two cell types. Reproduced under the terms of the Creative Commons Attribution 4.0 International License.<sup>[51]</sup> Copyright 2016, Macmillan Publishers Limited.

cell–cell interface, which resulted in the activation of downstream “cell differentiation” programs which in turn led to further sorting. The orchestrated use of cell sorting and cell–cell signaling modules created programmed self-organizing multilayered structures. These exhibit spherical symmetry or asymmetry depending on the design, are reversible, and show regeneration capabilities after being cut into two sections. Even more, by engineering antagonistic synNotch ligand/receptor pairs to perform lateral inhibition, a self-organizing 2-layered structure emerged from an initially undifferentiated population of isogenic cells.<sup>[50]</sup>

## 6. When Mechanical Forces Determine Patterning

The expansion of a confluent population of cells generates mechanical forces that can suffice to produce tree-like or fractal patterns (Figure 5A), as observed during airway branching or villi formation in the gut.<sup>[58,59]</sup> This patterning mechanism fully relies on physicomachanical forces and properties. Thus far, synthetic examples of such pattern formation based on mechanical forces were limited to a rather descriptive approach: labeling a growing population of rod-shaped bacteria with different fluorescent reporters was enough to obtain complex stochastic fractal patterns of the differentially labelled sub-populations (Figure 5B).<sup>[60,61]</sup> The overall pattern could be modified by using cells with different morphologies due to mutations in a cytoskeletal (MreB)<sup>[61]</sup> or a cell wall protein (RodA).<sup>[60]</sup> Rather than starting with multiple cells carrying different fluorescent reporters, this patterning mechanisms can also be started from a single founder lineage,<sup>[60,62]</sup> namely by exploiting the stochastic segregation of plasmids carrying distinct reporter proteins into different daughter cells.<sup>[60,62]</sup> This simple form

of spatial patterning might have potential in engineering more stable or productive synthetic microbial communities.<sup>[63]</sup>

## 7. The Elusive Turing Patterns

In his seminal article of 1952, the father of computation, Alan Turing, proposed a theoretical model of biological pattern formation in which repetitive patterns such as dots, stripes, and labyrinths could emerge in the absence of any pre-existing cue.<sup>[64]</sup> Two decades later, Gierer and Meinhardt further contributed to this model of self-organizing pattern formation.<sup>[65]</sup> The classical “Turing”, “Gierer–Meinhardt”, or “reaction–diffusion” model of pattern formation involves two diffusible species—one activator and one repressor. The activator favors the production of both itself and the repressor, while the repressor inhibits the production of the activator (Figure 6A). Small molecular fluctuations causing slightly higher levels of the activator in some cells will thus lead to higher levels of the activator and the repressor. A key necessary condition of this classical model is that the diffusion rate of the repressor needs to be considerably higher than that of the activator.<sup>[65,66]</sup> The positive feedback of the activator coupled to its low diffusivity subsequently drives its accumulation in local patches or islands, while the fast-diffusing repressor prevents the formation and coalescence of islands too close from each other.

The Turing mechanism is highly attractive for pattern formation, since a simple genetic network is able to produce de novo complex periodic patterns that self-repair when perturbed and in which the number of repeated motifs scales in response to changes in the tissue size. Turing systems have been proposed to play a role in the embryonic development of structural patterns (e.g., for limbs, hair follicles, and palate) as well as in animal coat patterns and skin pigmentation.<sup>[67–72]</sup>

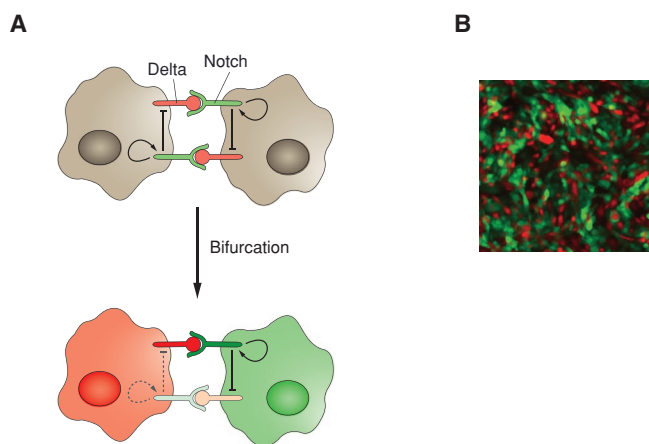


**Figure 4.** Lateral inhibition driven by the Delta–Notch ligand–receptor pair. A) Matsuda et al. developed a synthetic system that emulates natural Delta–Notch lateral inhibition. Binding of Delta to Notch triggers the cleavage of Notch and the release of its intracellular domain, which acts as a transcription factor that leads to downregulation of Delta and self-upregulation. Initially, the two adjacent cells have similar expression levels of the components. Noise-driven slight differences in expression levels are amplified by the lateral inhibition circuit, resulting in a complete bifurcation of cells into Delta-positive (Notch-negative) and Notch-positive (Delta-negative) cells. B) Implementation of the lateral inhibition circuit in mammalian cells led to a salt-and-pepper pattern of intermingled red (Delta-positive) and green (Notch-positive) cells. Reproduced with permission.<sup>[56]</sup> Copyright 2015, Springer Nature.

Interestingly, the high difference in diffusion rates between the two morphogens of the classical model is difficult to achieve in biological systems, and the parameter space (i.e., the number of parameter combinations) that allows for classical Turing

patterns is extremely narrow, practically unrealistic.<sup>[73,74]</sup> This is in apparent contradiction with the high number of Turing mechanisms proposed to underlie natural patterns, and may also explain why the construction of synthetic Turing patterns has remained elusive thus far despite the growing interest of synthetic biologists in pattern formation.<sup>[8,75–77]</sup>

Recently, Karig et al. engineered a self-organizing synthetic system in which an isogenic population of bacteria produced a 2D pattern of red fluorescent patches in a background of green fluorescence.<sup>[78]</sup> The responsible synthetic network topology consists of a two-node network in which two differentially diffusing homoserine lactones operate as an activator and a repressor and is thus reminiscent of a classical Turing network. However, this network does not function as a classical Turing system but rather as a “stochastic Turing system”<sup>[73]</sup> that produces patterns lacking many of the characteristic features of a classical Turing pattern, such as regularity in spot size, shape, intensity, and intervals. Indeed, these “stochastic” patterns cannot be captured by a deterministic Turing model, but require stochastic simulations.<sup>[73]</sup>

The recent work by Sekine et al. represents another notable effort toward the goal of engineering a synthetic Turing pattern.<sup>[79]</sup> Their synthetic network implemented in mammalian cells employs the well-characterized Nodal–Lefty pathway. The binding of Nodal to its receptor promotes the expression of both Nodal and Lefty, while Lefty inhibits Nodal signaling. Moreover, the diffusion of Nodal is significantly slower than that of Lefty. Thus, the proteins Nodal and Lefty satisfy the requirements for a classic Turing pattern. Indeed, the engineered (HEK) cells spontaneously display a pattern of Nodal-positive patches surrounded by Nodal-negative cells. However, the periodicity of this reaction–diffusion system is low, indicating that it is probably not a classical Turing pattern. Despite the indubitable

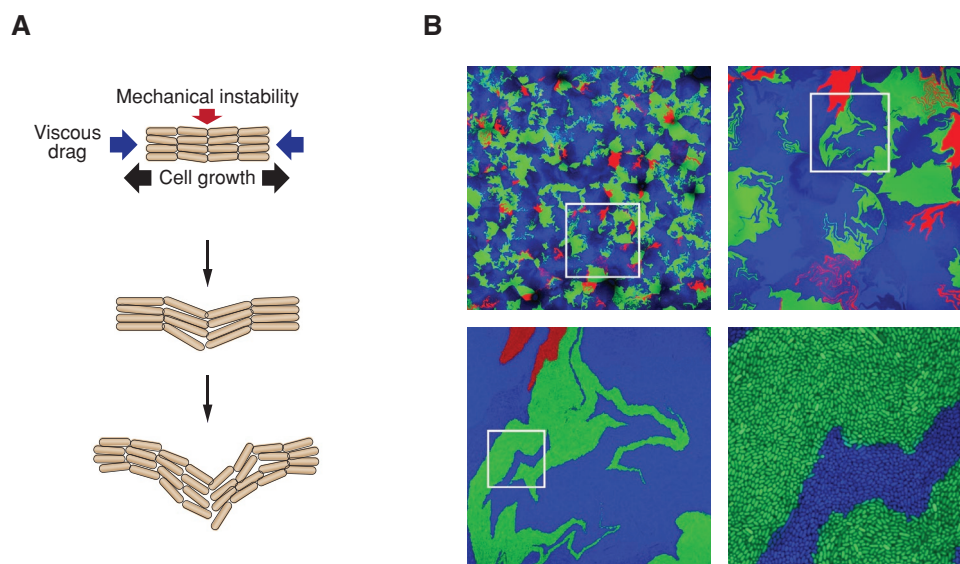


**Figure 5.** Formation of fractal patterns by mechanical forces in a population of rod-shaped bacteria. A) Top view of a monolayer of bacterial cells. Instabilities arising from cell growth and geometry are amplified over time as the confluent population expands, leading to fractal patterns. B) Surface growing *E. coli* labelled with three different fluorescent reporters form fractal patterns at the boundaries between confluent populations of cells. Reproduced with permission.<sup>[60]</sup> Copyright 2013, American Chemical Society.



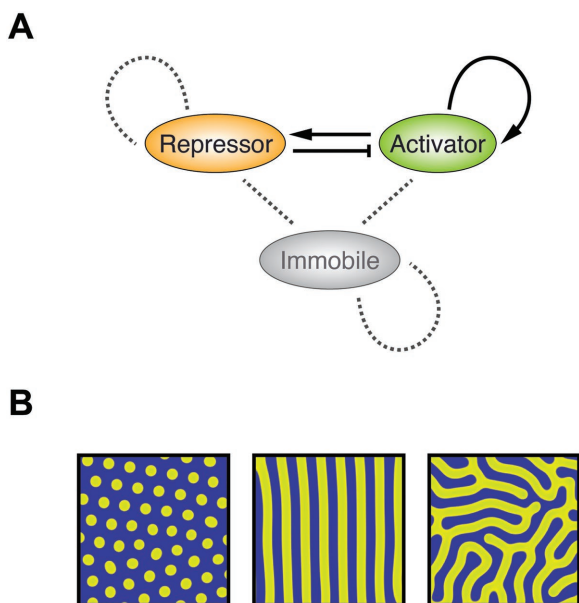


**Figure 6.** Turing pattern formation through a reaction–diffusion mechanism. A) The classical Turing model implies two diffusing species, a slow-diffusing activator and a fast-diffusing repressor.<sup>[64,65]</sup> The activator is subjected to a direct positive feedback loop, and an indirect negative feedback-loop through the action of the repressor. The diffusion coefficients of the two species are very different, which guarantees that clusters of the self-activating activator are surrounded by the repressor. Recent theoretical studies suggested that the inclusion of an additional immobile (non-diffusing) species may relax (or even suppress) the differential diffusivity requirement and allow for many more topologies (additional interactions represented as dotted lines).<sup>[68,74,80,82]</sup> B) Turing systems produce self-organizing (i.e., autonomous, independent of any external cue) regular patterns such as spots, stripes, and labyrinths. To date, no synthetic biological system has achieved genuine Turing patterns.

significance of these two recent studies and their contribution to the advancement in the field, the engineering of a genuine Turing system remains yet to be achieved.

However, recent theoretical studies have suggested that more network topologies than previously thought can produce Turing patterns<sup>[68,80–82]</sup> and that the differential diffusivity requirements may be relaxed (or even disappear) under certain conditions, for example, with increased cooperativity or when additional species are added to the classical two-species model.<sup>[66,68,74,82]</sup> While Turing only considered 2-node systems, networks with more than two nodes can generate Turing patterns through a mechanism that is analogous to the original 2-node case, and therefore these more complex systems are widely considered to be Turing systems.<sup>[68,74,80,82]</sup> For example, Marcon et al. predict that the addition of extra immobile (non-diffusing) nodes leads to Turing networks that do not require differential diffusivity and increases the number of topologies with the potential to create Turing patterns.<sup>[68]</sup> Furthermore, Diego et al. uncovered how network topology determines diffusivity constraints and provided a general mechanism for the removal of such constraints.<sup>[74]</sup> Together, these recent theoretical studies provide new frameworks to identify natural Turing patterns and to finally engineer synthetic systems displaying genuine Turing patterns.

## 8. Temporal Patterns Producing Spatial Patterns

In addition to the spatial patterning discussed so far, there exists another, perhaps less obvious but no less important form of biological patterning: temporal pattern formation. Oscillations constitute one of the most important forms of temporal patterns, being present in a myriad of biological systems and processes, such as the cell cycle, the circadian clock, energy metabolism, hormone secretion, cardiac function, or respiration.<sup>[83–85]</sup> Importantly, temporal rhythms can also produce (periodic) spatial patterns induced for example by spatially varying signals (morphogens).<sup>[86]</sup> Prominent examples include segmentation in developing short-germ insects<sup>[87]</sup> and somitogenesis in vertebrate embryos.<sup>[88]</sup> During the latter, an oscillating GRN (“segmentation clock”) is thought to be responsible for the sequential subdivision of the growing vertebrate embryo axis into segments (somites) which develop into the vertebral column. The “clock and wavefront” model is the dominant framework to explain this conversion of a temporal signal into a spatial pattern: the segmentation clock produces synchronized oscillations in the tissue and the morphogen “wavefront” travels through the tissue and arrests the oscillations as it advances.<sup>[89]</sup>

Since the landmark study of Elowitz and Leibler who built the first synthetic oscillator (the repressilator),<sup>[90]</sup> many synthetic oscillators with different designs and improved properties have been constructed. This body of work has already been extensively reviewed and we refer the reader to this literature.<sup>[91,92]</sup> Instead, we focus here on the (surprisingly) few studies in synthetic biology that looked at how temporal signals can lead to spatial patterns.

The repressilator connected the repressors TetR, cI, and LacI in a ring-like architecture giving rise to a “closed” cascade of repressing interactions.<sup>[90]</sup> The original version suffered from irregular oscillations that were displayed by only ≈40% of the engineered *E. coli* cells. Improved versions of the circuit addressed the main limitations of the original design to achieve robust oscillations that maintained population-level synchronous oscillation after initial synchronization without any form of cell–cell communication.<sup>[93,94]</sup> Oscillations of the repressilator are arrested when the *E. coli* cells slow down growth and enter stationary phase.<sup>[90]</sup> This happens presumably due to a decrease of available “housekeeping” sigma factor  $\sigma^{70}$  in stationary phase, which is required for RNA polymerase binding to the promoters of the repressilator.<sup>[92]</sup> Potvin-Trottier et al. took advantage of this feature to produce a spatial pattern at the scale of bacterial colonies: growing colonies of bacteria containing the improved repressilator circuit form a concentric multiring pattern of the fluorescent proteins used to visualize the expression dynamics of each network node (Figure 7). Cells at different radii of the colony enter stationary phase and arrest oscillations at different points of the oscillation phase. One could argue that the repressilator is working as a segmentation clock, while the transition to the stationary phase is playing the role of the wavefront (Figure 7).

Similarly, a synthetic circuit based on density-dependent motility built by Liu et al. also produces ring patterns in a growing colony.<sup>[41]</sup> The network is composed of two modules: a density-sensing module produces AHL and a motility-control

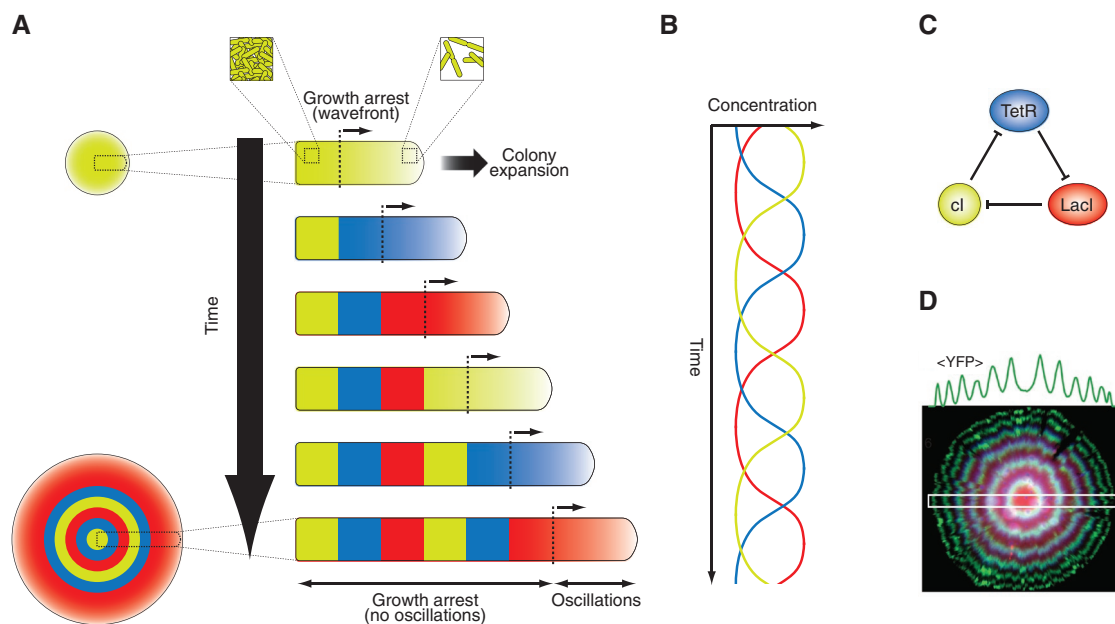


**Figure 7.** Temporal patterns translate into spatial arrangements. A population of cells with oscillating gene expression can form a periodic spatial pattern if a travelling wavefront “freezes” the clock at a given state as it advances (“clock and wavefront” model).<sup>[89]</sup> A) Schematics showing a bacterial population with oscillatory gene expression of “yellow”, “blue”, and “red” genes. As the colony expands, growing cells in the colony edge continue to oscillate, while cells in the colony center enter stationary phase, which ceases oscillations. The growth arrest here acts as a travelling wavefront, resulting in a periodic multiring patterns as the colony grows. B) Oscillatory expression of yellow, blue, and red genes as a function of time. C) Representation of the repressilator,<sup>[90]</sup> a synthetic oscillator. In the repressilator version of Potvin-Trottier et al.,<sup>[93]</sup> the expression of TetR, LacI, and cl repressors is monitored through CFP, RFP, and YFP fluorescent reporters, respectively. D) *E. coli* cells carrying the Potvin-Trottier repressilator form colonies with a tree-like ring pattern as a consequence of growth-driven clock arrest as the colony expands. Reproduced with permission.<sup>[93]</sup> Copyright 2016, Springer Nature.

module responds to high cell density (i.e., high AHL) by switching off chemotaxis-driven motility. Thus, as the colony grows AHL is produced and causes the cells to tumble and accumulate in place. Since AHL diffusion is limited, a few cells manage to escape the motility arrest, swim away, and begin the process again. The result is a pattern of concentric rings alternating bright (high cell density) and dark (low cell density) stripes.

While a delayed negative feedback as in the repressilator suffices to create oscillations, a network of interlinked negative and positive feedbacks can produce more robust and tunable oscillatory dynamics,<sup>[95]</sup> as well as other dynamical responses like bistability.<sup>[96]</sup> Various such “dual feedback” synthetic oscillators have been built by Hasty and co-workers.<sup>[97–100]</sup> In order to synchronize oscillations in a population of cells, Danino et al. complemented the dual feedback topology with quorum-sensing elements.<sup>[98]</sup> However, due to the relatively slow diffusion of AHL, the synchronization of oscillations with this circuit is limited to cells grown in the same microfluidic chamber (utilized to keep the cells continuously growing in exponential phase) with dimensions of about  $100 \times 100 \mu\text{m}^2$ . This scale limitation of synchronization leads to very interesting spatiotemporal dynamics over large (millimeter) scales: travelling waves emerge spontaneously due to small perturbations in the central chambers and propagate outward to cells growing in neighboring chambers of the microfluidic device.<sup>[98]</sup>

To extend the synchronization to centimeter-length scales, the local intracolony quorum sensing signaling was combined

with intercolony communication by fast-diffusing  $\text{H}_2\text{O}_2$  vapor.<sup>[99]</sup> In addition to producing completely synchronized oscillation over cm-scale surfaces (up to  $2.9 \text{ cm}^2$ ), this system is also capable of generating more complex spatiotemporal behaviors such as antiphase synchronization between neighboring colonies simply by manipulating the geometry of the microfluidic device harboring the cells, e.g., the distance between the individual chambers.

Bar-Ziv and co-workers employed another elegant approach to study how oscillatory reactions can produce spatial patterns: a cell-free transcription–translation system was set up on a microfluidic device in which compartments containing immobilized DNA were interconnected via diffusion.<sup>[101,102]</sup> Spatial patterns of alternating low and high GFP expression are generated if one of the genes of the oscillator network is expressed in a concentration gradient (achieved by localized DNA immobilization). Plotting these expression levels against time reveals checker-board spatiotemporal patterns. Additionally, spontaneous spatiotemporal patterns can also be induced by fluctuations in the absence of a concentration gradient. As in the microfluidic array of compartments for long-range synchronous oscillations,<sup>[99]</sup> in this setup the dynamic system can also be controlled by the geometry of the microfluidic device, which influences the coupling between the oscillating compartments.

In summary, synthetic biologist have started to build systems that use temporal patterns to generate spatial patterns and can be used to reveal the underlying design principles. However, there is still a lot of work ahead of us until we can rival natural spatiotemporal patterning systems.

## 9. Pattern Formation Controlled by Light

Optogenetics, i.e., the use of light to precisely control molecular events, constitutes a valuable tool for synthetic pattern formation. Light-controlled patterning systems often allow for a great complexity of the output pattern. Importantly, the studies presented below differ from the patterning forms discussed above in that they reproduce (rather than produce) a pattern, i.e., the complex output is a reflection of an equally complex input. This lack of self-organization, however, does not hamper their utility: the high spatial and temporal resolution of light excitation provides a level of induction accuracy that is hardly achievable with chemical inducer signals, and photoactivated molecular changes are commonly reversible upon light source removal.<sup>[103,104]</sup>

The Voigt lab has pioneered the interfacing of light-detecting modules with downstream networks that allow bacterial populations to adopt color patterns in response to (pre-patterned) light cues. In 2005, they developed a chimeric photoreceptor that repressed the downstream production of a black pigment upon red light excitation. When using a non-homogeneous (“patterned”) light source for excitation, a 2D population of the engineered bacteria was able to capture the details of the input light signal as a black and white biological “photograph”.<sup>[105]</sup> Few years later, they modified the aforementioned dark sensor to repurpose it for edge-detection.<sup>[106]</sup> Basically, the new design connected dark detection to the production of two antagonistic molecules: AHL, which diffuses across cells and activates pigment synthesis, and the cI repressor, which blocks pigment production intracellularly in cells grown in the dark. Therefore, only cells within the light-exposed region but close enough to the dark area were able to synthesize the pigment induced by AHL. Interestingly, while in silico edge-detection algorithms suffer from linearly increasing computation times with increasing number of pixels, the bacterial edge-detection system implements a parallel computation that is independent of image size. Recently, they took light-dictated patterning a step further and developed a complex (18-gene) circuit that generates colored bacterial “photographs” in response to red, green, and blue light (Figure 8A).<sup>[107]</sup>

Instead of using light to pattern a homogeneous layer of cells, optogenetic control can also be employed to modulate the patterned adhesion of cells to a surface. Light can for example be used to control receptor–ligand dimerization or adhesin gene expression. Photoswitchable cell adhesion systems have been developed in bacteria and eukaryotes to control surface attachment of cells in a pattern.<sup>[109–111]</sup> A dynamic version of light-dictated spatial cell arrangement is that of photokinetic *E. coli*. These minimally engineered bacteria produce proteorhodopsin, a proton pump that contributes to the electrochemical gradient across the inner membrane upon light exposure. In swimming bacteria, where the proton motive force powers the rotation of the flagellar motor, cells swim more rapidly in light-exposed areas and accumulate in dark regions, which allows the formation of complex dynamic spatial patterns just by controlling local cell density through differential illumination of the field (Figure 8B).<sup>[108,112]</sup>

A



B



**Figure 8.** Light-controlled patterns. A) Complex RGB (“red, green, blue”) bacterial “picture” as a result of patterned incident light (inset) that triggers pigment production in a population of engineered *E. coli* cells. Reproduced with permission.<sup>[107]</sup> Copyright 2017, Springer Nature. B) A projected image on a population of *E. coli* designed to swim in a light-dependent manner modifies their local density such as to create “grayscale” dynamic patterns that mirror the incident image. Shown is the time-averaged density profile over 6 min. Reproduced under the terms of the Creative Commons Attribution 4.0 International License.<sup>[108]</sup> Copyright 2018, The Authors, published by eLife.

## 10. Conclusions and Perspectives

Synthetic biology adopts an engineering approach to build artificial systems based on natural counterparts. “Classical” research in biology applies a top-down, reverse engineering strategy: different parts of a complex system are perturbed to deduce their function; the sum or combination of complementary pieces of evidence allow researchers to infer a general picture of the system as a whole. Conversely, synthetic biology relies on a bottom-up, forward engineering approach in which, starting from basic constituent parts, more or less simple systems are assembled together to (roughly) mimic a natural system or to explore non-natural solutions.

The use of a synthetic biology approach to build and study patterning systems has proven greatly successful so far. Yet, exciting challenges remain that will likely be addressed in the short- or mid-term. One of the missing pieces in the synthetic patterning toolbox that might be added in the near future is

that of a synthetic Turing pattern. While Turing patterns have been achieved in purely chemical systems,<sup>[113–118]</sup> a synthetic implementation of a genuine Turing pattern in a biological system is yet to come. The labs of Weiss and Ebisuya have recently published self-organizing systems that are reminiscent of a canonical Turing system but lack some of its distinctive features.<sup>[78,79]</sup> As opposed to the classical conception of the Turing mechanism, which depicted a very limited parameter space allowing for patterning, recent theoretical studies suggest that Turing patterns may not actually be so demanding, especially in network designs with more than two nodes.<sup>[68,74,82]</sup> Therefore, future attempts to engineer biological Turing systems may not focus on two-node networks with high parameter sensitivity, but will presumably explore the recently proposed more complex and robust network topologies.<sup>[68,74,80,82]</sup>

More complex patterns than those achieved so far are also desirable. Pattern complexity does not necessarily correlate with GRN complexity—Turing systems, for example, generate complex patterns out of fairly simple underlying networks. However, complex patterning can also be achieved by combining simple patterning modules into a higher-order network. For instance, a theoretical study on patterning network connectivity showed that the output (stripe pattern) of stripe-forming networks can be used as input by a downstream stripe-forming network, giving rise to a multistripe pattern.<sup>[119]</sup>

Multifunctional GRNs may provide another route toward controlling complex spatiotemporal patterns, while keeping the synthetic circuit small. Multifunctional circuits are capable of exhibiting qualitatively different behaviors depending on the conditions.<sup>[120–123]</sup> For example, the AC–DC circuit<sup>[124,125]</sup> is a combination of the toggle switch<sup>[126]</sup> and the repressilator<sup>[90]</sup> and owes its name to its ability to exhibit oscillatory (AC: alternate current) and multistable switch-like (DC: direct current) expression patterns. This combination results in emergent properties not displayed by any of the two subnetworks, such as fast on/off switching of synchronous oscillations and the spatial propagation of signals.<sup>[122]</sup>

Ideally, a prospective higher level of pattern complexity should not be accompanied by an increase in the complexity of the input signal(s). Not all patterning mechanisms allow for the same degree of autonomy (Turing patterns are self-organizing, i.e., input-independent, while French flag-based systems require an input gradient), but patterns with highly complex inputs provide poor information gain: much of the complexity of the final pattern is already encoded in the input signal.

Another source of novel and more complex patterns may emerge from combining different patterning mechanisms. In natural systems, the boundaries between different patterning mechanisms are presumably loose, even though for the sake of conceptualization and analysis researchers try to delimit patterning modules within a defined category. For example, the digit patterning in the mouse embryo is controlled by a combination of an early gradient of the sonic hedgehog morphogen, which establishes the anteroposterior polarity of the limb bud,<sup>[127]</sup> and a subsequent three-node Turing network (involving BMP, Sox9, and WNT) that positions a periodic digit pattern.<sup>[67]</sup> While most synthetic patterning designs rely on a single mechanism, Toda et al. combined two patterning mechanisms (phase separation and lateral inhibition),<sup>[50]</sup> and

we believe that in the future other studies will follow the same direction, which may allow us to better emulate natural processes and to broaden the synthetic patterning palette.

As highlighted above, synthetic biology allows us to tackle longstanding biological questions from a new angle, thus providing a valuable complementary approach to classical top-down research. While the classical biological research informs us about how particular natural phenomena work, the construction of synthetic counterparts of complex natural systems can be extremely informative with respect to the underlying regulatory networks and general design principles. This is also true for synthetic systems emulating natural patterning processes. A beautiful example is found in a recent work from Elowitz and co-workers, in which the reconstitution of the Hedgehog gradient showed that the design of the natural pathway accelerates gradient formation and increases robustness to variations in ligand levels.<sup>[128]</sup> In another work, Delta–Notch driven lateral inhibition was studied using a minimal network that showed, for instance, that bifurcation into Delta-positive and Delta-negative cells is spontaneous, robust, and static rather than dynamic, and that Lunatic fringe (Lfng) participates in a sub-circuit that causes bimodal distribution even when the main Delta–Notch inhibition is absent.<sup>[56]</sup>

Synthetic systems have also been used to demonstrate that a specific network or mechanism is capable to generate a pattern of interest. For example, all four IFFLs have been built synthetically and shown to form a stripe in a concentration gradient.<sup>[19,24,28–40]</sup> However, to the best of our knowledge, only I1 and I2 have so far been observed in natural stripe-forming systems.<sup>[21]</sup> Natural systems using the I3 and I4 networks might be discovered in future, or a synthetic system might be used to unveil properties that make them less likely to appear in the repertoire of natural stripe-forming networks. Similarly, the work of Cao et al. using a morphogen-independent artificial system suggests a potential mechanism for pattern generation and scaling in nature.<sup>[43]</sup> Finally, the understanding of how physicochemical laws determine patterning (for example, during bacterial colony formation, or in adhesion-driven phase separation) has also benefitted from the building and examination of controllable synthetic systems.<sup>[48,51,52,60–62]</sup>

The ability to build, understand, and modify synthetic patterns may enable their use as a tool to study, with a new perspective, not only patterning events but also other varied biological problems. For instance, stripe-forming networks have recently been employed to address questions of GRN evolution.<sup>[129]</sup> Two incoherent feed-forward loops (I2 and I3) producing the same phenotype (a stripe) through different regulatory mechanisms were used to study mutations that cause novel phenotypes. Experimental measurements, mathematical modeling, and DNA sequencing were combined to show that the regulatory mechanism of a network restricts the possible phenotypic variation upon mutation.

Although most of the work discussed here is basic research, synthetic patterns also have potential applications, for example, in tissue engineering. Tissue engineering aims to create tissues and organs outside the developing embryo. The thus obtained structures are interesting disease and drug-screening models and can be used to repair or replace damaged tissues and organs in regenerative medicine.<sup>[130]</sup> Controlling patterning



and cell differentiation is one of the main challenges of tissue engineering. Traditionally, tissue engineers rely either on the intrinsic self-organizing properties of the (stem) cells employed and/or on templated structures (e.g., obtained by 3D printing) seeded with living cells to obtain a specific arrangement.<sup>[131]</sup>

The combination of these approaches with the tools of synthetic biology to control cell differentiation and pattern formation promises to provide unprecedented control for programming the generation of complex tissues and organs. For example, Guye et al. obtained a complex liver-bud-like structure from a genetically engineered human induced pluripotent stem cells (hiPSC) expressing different levels of a transcription factor (GATA6).<sup>[132]</sup> Similarly, hiPSC were guided through sequential differentiation steps up to an insulin-secreting beta-like phenotype by a synthetic network engineered to respond to input levels of the food additive vanillic acid and translate this signal into a precise temporal control of gene expression.<sup>[39]</sup> The excitement for this “synthetic tissue development” or “synthetic morphogenesis” is reflected by a row of recent reviews to which we refer to.<sup>[133–138]</sup>

Another field that can greatly benefit from controllable patterning capabilities to create nonhomogeneous products is that of bioderived material production.<sup>[139]</sup> For example, bacterial curli fibers, involved in biofilm formation, are suitable carriers for surface display of custom molecules due to their simple secretory mechanism.<sup>[140]</sup> The labelling of curli with conductive elements, e.g., gold nanoparticles, provides colonies with electrical conductance and allowed to build bacterial pressure sensors.<sup>[44]</sup> Finally, biotechnological processes may also take advantage of spatiotemporal patterns, which could facilitate the channeling of reaction intermediates through the production flux.<sup>[141,142]</sup>

So far, the majority of synthetic patterning systems used bacterial host cells. The possibility to use unicellular organisms to understand the underlying principles of multicellular organism development is one of the advantages of the synthetic biology approach. However, in the light of applications in tissue engineering, synthetic patterning of eukaryotic cells<sup>[35,38,39,48,50–52,56,79,132,143]</sup> promises to gain in relevance in the following years. Most tissue engineering applications will likely require 3D patterns<sup>[50]</sup> rather than 2D configurations, and therefore efforts should be made in the third dimension.

Despite the excitement and indubitable potential of synthetic patterning, the field suffers from the same limitations that synthetic biologists face in general: the particularities and complexity of life makes that desirable goals such as predictability, standardization, robustness, or modularity are difficult to achieve to the same extent as in other engineering disciplines.<sup>[144,145]</sup> Nevertheless, intrinsic challenges of the field should not discourage synthetic biologists, and efforts should be made that bring us as close as possible to these goals. During the 2000s and the 2010s synthetic biology has experienced a remarkable boom both in basic and applied research.<sup>[1–7]</sup> In future further advances are expected, also boosted by technological progress such as CRISPR<sup>[146]</sup> and optogenetics,<sup>[147]</sup> or dropping costs in DNA synthesis.

The combination of synthetic and developmental biology is proving to be a fruitful partnership.<sup>[8,77,134,135]</sup> As showcased in this Progress Report, the application of synthetic biology

to patterning has already produced promising results. In the future, the synergistic combination of cutting-edge technology and engineered cell-organization control promises to deliver exciting fundamental insights into the principles of pattern formation and their applications in market-ready products.

## Acknowledgements

The authors thank Florian Baier, Christian Cuba Samaniego, Xavier Diego, and Luciano Marcon for critical reading and valuable feedback. Y.S. acknowledges support by the Swiss National Science Foundation grant 31003A\_175608.

## Conflict of Interest

The authors declare no conflict of interest.

## Keywords

bottom-up approach, developmental biology, pattern formation, spatial patterns, synthetic biology

Received: September 28, 2018

Revised: November 14, 2018

Published online:

- [1] D. E. Cameron, C. J. Bashor, J. J. Collins, *Nat. Rev. Microbiol.* **2014**, *12*, 381.
- [2] C. J. Bashor, J. J. Collins, *Annu. Rev. Biophys.* **2018**, *47*, 399.
- [3] G. M. Church, M. B. Elowitz, C. D. Smolke, C. A. Voigt, R. Weiss, *Nat. Rev. Mol. Cell Biol.* **2014**, *15*, 289.
- [4] M. Q. Xie, M. Fussenegger, *Nat. Rev. Mol. Cell Biol.* **2018**, *19*, 507.
- [5] T. Kitada, B. DiAndreth, B. Teague, R. Weiss, *Science* **2018**, *359*, eaad1067.
- [6] J. Nielsen, J. D. Keasling, *Cell* **2016**, *164*, 1185.
- [7] R. A. Le Feuvre, N. S. Scrutton, *Synth. Syst. Biotechnol.* **2018**, *3*, 105.
- [8] J. Davies, *Development* **2017**, *144*, 1146.
- [9] J. K. Polka, S. G. Hays, P. A. Silver, *Cold Spring Harbor Perspect. Biol.* **2016**, *8*, a024018.
- [10] T. Xu, S. Petridou, E. H. Lee, E. A. Roth, N. R. Vyavahare, J. J. Hickman, T. Boland, *Biotechnol. Bioeng.* **2004**, *85*, 29.
- [11] J. Merrin, S. Leibler, J. S. Chuang, *PLoS One* **2007**, *2*, e663.
- [12] A. S. Zadorin, Y. Rondelez, G. Gines, V. Dilhas, G. Urtel, A. Zambrano, J. C. Galas, A. Estevez-Torres, *Nat. Chem.* **2017**, *9*, 990.
- [13] S. Kretschmer, L. Harrington, P. Schwill, *Philos. Trans. R. Soc., B* **2018**, *373*, 20170104.
- [14] D. Gilmour, M. Rembold, M. Leptin, *Nature* **2017**, *541*, 311.
- [15] D. Papatsenko, *BioEssays* **2009**, *31*, 1172.
- [16] J. Briscoe, S. Small, *Development* **2015**, *142*, 3996.
- [17] A. D. Lander, *Cell* **2007**, *128*, 245.
- [18] L. Wolpert, *Curr. Top. Dev. Biol.* **1971**, *6*, 183.
- [19] Y. Schaefer, A. Munteanu, M. Gili, J. Cotterell, J. Sharpe, M. Isalan, *Nat. Commun.* **2014**, *5*, 4905.
- [20] G. Rodrigo, S. F. Elena, *PLoS One* **2011**, *6*, e16904.
- [21] J. Cotterell, J. Sharpe, *Mol. Syst. Biol.* **2010**, *6*, 425.
- [22] P. Francois, E. D. Siggia, *Development* **2010**, *137*, 2385.
- [23] S. Mangan, U. Alon, *Proc. Natl. Acad. Sci. USA* **2003**, *100*, 11980.

- [24] R. Entus, B. Aufderheide, H. M. Sauro, *Syst. Synth. Biol.* **2007**, *1*, 119.
- [25] M. Lynch, G. K. Marinov, *Proc. Natl. Acad. Sci. USA* **2015**, *112*, E30.
- [26] F. Ceroni, R. Algar, G. B. Stan, T. Ellis, *Nat. Methods* **2015**, *12*, 415.
- [27] F. Ceroni, A. Boo, S. Furini, T. E. Gorochoowski, O. Borkowski, Y. N. Ladak, A. R. Awan, C. Gilbert, G. B. Stan, T. Ellis, *Nat. Methods* **2018**, *15*, 387.
- [28] S. Basu, Y. Gerchman, C. H. Collins, F. H. Arnold, R. Weiss, *Nature* **2005**, *434*, 1130.
- [29] Y. Schaeferli, M. Gili, M. Isalan, *Nucleic Acids Res.* **2014**, *42*, 12322.
- [30] A. Buetti-Dinh, R. Ungricht, J. Z. Kelemen, C. Shetty, P. Ratna, A. Becskei, *Mol. Syst. Biol.* **2009**, *5*, 300.
- [31] M. Isalan, C. Lemerle, L. Serrano, *PLoS Biol.* **2005**, *3*, e64.
- [32] T. Ellis, X. Wang, J. J. Collins, *Nat. Biotechnol.* **2009**, *27*, 465.
- [33] T. Sohka, R. A. Heins, R. M. Phelan, J. M. Greisler, C. A. Townsend, M. Ostermeier, *Proc. Natl. Acad. Sci. USA* **2009**, *106*, 10135.
- [34] T. Sohka, R. A. Heins, M. Ostermeier, *J. Biol. Eng.* **2009**, *3*, 10.
- [35] D. Greber, M. Fussenegger, *Nucleic Acids Res.* **2010**, *38*, e174.
- [36] N. Muranaka, Y. Yokobayashi, *Chem. Commun.* **2010**, *46*, 6825.
- [37] N. Muranaka, Y. Yokobayashi, *Angew. Chem., Int. Ed.* **2010**, *49*, 4653.
- [38] M. M. Kampf, R. Engesser, M. Busacker, M. Horner, M. Karlsson, M. D. Zurbriggen, M. Fussenegger, J. Timmer, W. Weber, *Mol. Biosyst.* **2012**, *8*, 1824.
- [39] P. Saxena, B. C. Heng, P. Bai, M. Folcher, H. Zulewski, M. Fussenegger, *Nat. Commun.* **2016**, *7*, 11247.
- [40] W. Kong, A. E. Blanchard, C. Liao, T. Lu, *Nucleic Acids Res.* **2017**, *45*, 1005.
- [41] C. Liu, X. Fu, L. Liu, X. Ren, C. K. Chau, S. Li, L. Xiang, H. Zeng, G. Chen, L. H. Tang, P. Lenz, X. Cui, W. Huang, T. Hwa, J. D. Huang, *Science* **2011**, *334*, 238.
- [42] S. Payne, B. Li, Y. Cao, D. Schaeffer, M. D. Ryser, L. You, *Mol. Syst. Biol.* **2014**, *9*, 697.
- [43] Y. Cao, M. D. Ryser, S. Payne, B. Li, C. V. Rao, L. You, *Cell* **2016**, *165*, 620.
- [44] Y. Cao, Y. Feng, M. D. Ryser, K. Zhu, G. Herschlag, C. Cao, K. Marusak, S. Zauscher, L. You, *Nat. Biotechnol.* **2017**, *35*, 1087.
- [45] C. R. Boehm, P. K. Grant, J. Haseloff, *Nat. Commun.* **2018**, *9*, 776.
- [46] E. Nudler, A. S. Mironov, *Trends Biochem. Sci.* **2004**, *29*, 11.
- [47] M. S. Steinberg, *Science* **1963**, *141*, 401.
- [48] R. A. Foty, M. S. Steinberg, *Dev. Biol.* **2005**, *278*, 255.
- [49] U. Tepass, D. Godt, R. Winklbauer, *Curr. Opin. Genet. Dev.* **2002**, *12*, 572.
- [50] S. Toda, L. R. Blauch, S. K. Y. Tang, L. Morsut, W. A. Lim, *Science* **2018**, *361*, 156.
- [51] E. Cachat, W. Liu, K. C. Martin, X. Yuan, H. Yin, P. Hohenstein, J. A. Davies, *Sci. Rep.* **2016**, *6*, 20664.
- [52] E. Cachat, W. Liu, J. A. Davies, *Eng. Biol.* **2017**, *1*, 71.
- [53] D. S. Glass, I. H. Riedel-Kruse, *Cell* **2018**, *174*, 649.
- [54] J. R. Collier, N. A. Monk, P. K. Maini, J. H. Lewis, *J. Theor. Biol.* **1996**, *183*, 429.
- [55] T. Pierfelice, L. Alberi, N. Gaiano, *Neuron* **2011**, *69*, 840.
- [56] M. Matsuda, M. Koga, K. Woltjen, E. Nishida, M. Ebisuya, *Nat. Commun.* **2015**, *6*, 6195.
- [57] L. Morsut, K. T. Roybal, X. Xiong, R. M. Gordley, S. M. Coyle, M. Thomson, W. A. Lim, *Cell* **2016**, *164*, 780.
- [58] V. D. Varner, J. P. Gleghorn, E. Miller, D. C. Radisky, C. M. Nelson, *Proc. Natl. Acad. Sci. USA* **2015**, *112*, 9230.
- [59] A. E. Shyer, T. Tallinen, N. L. Nerurkar, Z. Wei, E. S. Gil, D. L. Kaplan, C. J. Tabin, L. Mahadevan, *Science* **2013**, *342*, 212.
- [60] T. J. Rudge, F. Federici, P. J. Steiner, A. Kan, J. Haseloff, *ACS Synth. Biol.* **2013**, *2*, 705.
- [61] W. P. Smith, Y. Davit, J. M. Osborne, W. Kim, K. R. Foster, J. M. Pitt-Francis, *Proc. Natl. Acad. Sci. USA* **2017**, *114*, E280.
- [62] I. N. Nunez, T. F. Matute, I. D. Del Valle, A. Kan, A. Choksi, D. Endy, J. Haseloff, T. J. Rudge, F. Federici, *ACS Synth. Biol.* **2017**, *6*, 256.
- [63] T. Großkopf, O. S. Soyer, *Curr. Opin. Microbiol.* **2014**, *18*, 72.
- [64] A. M. Turing, *Philos. Trans. R. Soc., B* **1952**, *237*, 37.
- [65] A. Gierer, H. Meinhardt, *Kybernetik* **1972**, *12*, 30.
- [66] L. Diambra, V. R. Senthivel, D. B. Menendez, M. Isalan, *ACS Synth. Biol.* **2015**, *4*, 177.
- [67] J. Raspopovic, L. Marcon, L. Russo, J. Sharpe, *Science* **2014**, *345*, 566.
- [68] L. Marcon, X. Diego, J. Sharpe, P. Muller, *eLife* **2016**, *5*, e14022.
- [69] S. Sick, S. Reinker, J. Timmer, T. Schlake, *Science* **2006**, *314*, 1447.
- [70] A. D. Economou, A. Ohazama, T. Porntaveetus, P. T. Sharpe, S. Kondo, M. A. Basson, A. Gritli-Linde, M. T. Cobourne, J. B. Green, *Nat. Genet.* **2012**, *44*, 348.
- [71] A. Nakamasu, G. Takahashi, A. Kanbe, S. Kondo, *Proc. Natl. Acad. Sci. USA* **2009**, *106*, 8429.
- [72] L. Manukyan, S. A. Montandon, A. Fofonjka, S. Smirnov, M. C. Milinkovitch, *Nature* **2017**, *544*, 173.
- [73] T. Butler, N. Goldenfeld, *Phys. Rev. E* **2011**, *84*, 011112.
- [74] X. Diego, L. Marcon, P. Müller, J. Sharpe, *Phys. Rev. X* **2018**, *8*, 021071.
- [75] C. Liu, X. Fu, J.-D. Huang, *Quant. Biol.* **2013**, *1*, 246.
- [76] B. Borek, J. Hasty, L. Tsimring, *PLoS One* **2016**, *11*, e0153679.
- [77] N. S. Scholes, M. Isalan, *Curr. Opin. Chem. Biol.* **2017**, *40*, 1.
- [78] D. Karig, K. M. Martini, T. Lu, N. A. DeLateur, N. Goldenfeld, R. Weiss, *Proc. Natl. Acad. Sci. USA* **2018**, *115*, 6572.
- [79] R. Sekine, T. Shibata, M. Ebisuya, *bioRxiv* **2018**, <https://doi.org/10.1101/372490>.
- [80] N. S. Scholes, D. Schnoerr, M. Isalan, M. P. H. Stumpf, *bioRxiv* **2018**, <https://doi.org/10.1101/352302>.
- [81] S. Smith, N. Dalchau, arXiv:1803.07886v1.
- [82] M. M. Zheng, B. Shao, Q. Ouyang, *J. Theor. Biol.* **2016**, *408*, 88.
- [83] L. Glass, *Nature* **2001**, *410*, 277.
- [84] X. Zheng, A. Sehgal, *Genetics* **2008**, *178*, 1147.
- [85] B. Hess, *Naturwissenschaften* **2000**, *87*, 199.
- [86] A. B. Webb, A. C. Oates, *Dev., Growth Differ.* **2016**, *58*, 43.
- [87] N. H. Patel, *Development* **1994**, *201*.
- [88] A. C. Oates, L. G. Morelli, S. Ares, *Development* **2012**, *139*, 625.
- [89] J. Cooke, E. C. Zeeman, *J. Theor. Biol.* **1976**, *58*, 455.
- [90] M. B. Elowitz, S. Leibler, *Nature* **2000**, *403*, 335.
- [91] Z. Li, Q. Yang, *Quant. Biol.* **2018**, *6*, 1.
- [92] O. Purcell, N. J. Savery, C. S. Grierson, M. di Bernardo, J. R. Soc., *Interface* **2010**, *7*, 1503.
- [93] L. Potvin-Trottier, N. D. Lord, G. Vinnicombe, J. Paulsson, *Nature* **2016**, *538*, 514.
- [94] H. Niederholtmeyer, Z. Z. Sun, Y. Hori, E. Yeung, A. Verpoorte, R. M. Murray, S. J. Maerkl, *eLife* **2015**, *4*, e09771.
- [95] T. Y. C. Tsai, Y. S. Choi, W. Z. Ma, J. R. Pomeroy, C. Tang, J. E. Ferrell, *Science* **2008**, *321*, 126.
- [96] M. R. Atkinson, M. A. Savageau, J. T. Myers, A. J. Ninfa, *Cell* **2003**, *113*, 597.
- [97] J. Stricker, S. Cookson, M. R. Bennett, W. H. Mather, L. S. Tsimring, J. Hasty, *Nature* **2008**, *456*, 516.
- [98] T. Danino, O. Mondragon-Palomino, L. Tsimring, J. Hasty, *Nature* **2010**, *463*, 326.
- [99] A. Prindle, P. Samayoa, I. Razinkov, T. Danino, L. S. Tsimring, J. Hasty, *Nature* **2012**, *481*, 39.
- [100] M. O. Din, T. Danino, A. Prindle, M. Skalak, J. Selimkhanov, K. Allen, E. Julio, E. Atolia, L. S. Tsimring, S. N. Bhatia, J. Hasty, *Nature* **2016**, *536*, 81.
- [101] A. M. Tayar, E. Karzbrun, V. Noireaux, R. H. Bar-Ziv, *Proc. Natl. Acad. Sci. USA* **2017**, *114*, 11609.
- [102] E. Karzbrun, A. M. Tayar, V. Noireaux, R. H. Bar-Ziv, *Science* **2014**, *345*, 829.

- [103] A. Baumschlager, S. K. Aoki, M. Khammash, *ACS Synth. Biol.* **2017**, *6*, 2157.
- [104] M. Rullan, D. Benzinger, G. W. Schmidt, A. Miliars-Argeitis, M. Khammash, *Mol. Cell* **2018**, *70*, 745.
- [105] A. Levskaya, A. A. Chevalier, J. J. Tabor, Z. B. Simpson, L. A. Lavery, M. Levy, E. A. Davidson, A. Scouras, A. D. Ellington, E. M. Marcotte, C. A. Voigt, *Nature* **2005**, *438*, 441.
- [106] J. J. Tabor, H. M. Salis, Z. B. Simpson, A. A. Chevalier, A. Levskaya, E. M. Marcotte, C. A. Voigt, A. D. Ellington, *Cell* **2009**, *137*, 1272.
- [107] J. Fernandez-Rodriguez, F. Moser, M. Song, C. A. Voigt, *Nat. Chem. Biol.* **2017**, *13*, 706.
- [108] G. Frangipane, D. Dell'Arciprete, S. Petracchini, C. Maggi, F. Saglimbeni, S. Bianchi, G. Vizsnyiczai, M. L. Bernardini, R. Di Leonardo, *eLife* **2018**, *7*, e36608.
- [109] F. Chen, S. V. Wegner, *ACS Synth. Biol.* **2017**, *6*, 2170.
- [110] X. Jin, I. H. Riedel-Kruse, *Proc. Natl. Acad. Sci. USA* **2018**, *115*, 3698.
- [111] S. G. Yüz, J. Ricken, S. V. Wegner, *Adv. Sci.* **2018**, *5*, 1800446.
- [112] J. Arlt, V. A. Martinez, A. Dawson, T. Pilizota, W. C. K. Poon, *Nat. Commun.* **2018**, *9*, 768.
- [113] V. V. Castets, E. Dulos, J. Boissonade, P. De Kepper, *Phys. Rev. Lett.* **1990**, *64*, 2953.
- [114] Q. Ouyang, H. L. Swinney, *Nature* **1991**, *352*, 610.
- [115] K. Agladze, E. Dulos, P. De Kepper, *J. Phys. Chem.* **1992**, *96*, 2400.
- [116] J. Horvath, I. Szalai, P. De Kepper, *Science* **2009**, *324*, 772.
- [117] D. Feldman, R. Nagao, T. Bansagi Jr., I. R. Epstein, M. Dolnik, *Phys. Chem. Chem. Phys.* **2012**, *14*, 6577.
- [118] H. Liu, J. A. Pojman, Y. Zhao, C. Pan, J. Zheng, L. Yuan, A. K. Horvath, Q. Gao, *Phys. Chem. Chem. Phys.* **2012**, *14*, 131.
- [119] S. Ishihara, K. Fujimoto, T. Shibata, *Genes Cells* **2005**, *10*, 1025.
- [120] O. Purcell, M. di Bernardo, C. S. Grierson, N. J. Savery, *PLoS One* **2011**, *6*, e16140.
- [121] A. Jimenez, J. Cotterell, A. Munteanu, J. Sharpe, *Mol. Syst. Biol.* **2017**, *13*, 925.
- [122] R. Perez-Carrasco, C. P. Barnes, Y. Schaerli, M. Isalan, J. Briscoe, K. M. Page, *Cell Syst.* **2018**, *6*, 521.
- [123] G. Rodrigo, J. Carrera, S. F. Elena, A. Jaramillo, *BMC Syst. Biol.* **2010**, *4*, 48.
- [124] J. Panovska-Griffiths, K. M. Page, J. Briscoe, *J. R. Soc., Interface* **2012**, *10*, 20120826.
- [125] N. Balaskas, A. Ribeiro, J. Panovska, E. Dessaud, N. Sasai, K. M. Page, J. Briscoe, V. Ribes, *Cell* **2012**, *148*, 273.
- [126] T. S. Gardner, C. R. Cantor, J. J. Collins, *Nature* **2000**, *403*, 339.
- [127] J. J. Zhu, E. Nakamura, M. T. Nguyen, X. Z. Bao, H. Akiyama, S. Mackem, *Dev. Cell* **2008**, *14*, 624.
- [128] P. Li, J. S. Markson, S. Wang, S. Chen, V. Vachharajani, M. B. Elowitz, *Science* **2018**, *360*, 543.
- [129] Y. Schaerli, A. Jimenez, J. M. Duarte, L. Mihajlovic, J. Renggli, M. Isalan, J. Sharpe, A. Wagner, *Mol. Syst. Biol.* **2018**, *14*, e8102.
- [130] A. Shafiee, A. Atala, *Annu. Rev. Med.* **2017**, *68*, 29.
- [131] E. S. Place, N. D. Evans, M. M. Stevens, *Nat. Mater.* **2009**, *8*, 457.
- [132] P. Guye, M. R. Ebrahimkhani, N. Kipniss, J. J. Velazquez, E. Schoenfeld, S. Kiani, L. G. Griffith, R. Weiss, *Nat. Commun.* **2016**, *7*, 10243.
- [133] M. B. Johnson, A. R. March, L. Morsut, *Curr. Opin. Biomed. Eng.* **2017**, *4*, 163.
- [134] J. A. Davies, E. Cachat, *Biochem. Soc. Trans.* **2016**, *44*, 696.
- [135] B. P. Teague, P. Guye, R. Weiss, *Cold Spring Harbor Perspect. Biol.* **2016**, *8*, a023929.
- [136] A. Ollé-Vila, S. Duran-Nebreda, N. Conde-Pueyo, R. Montañez, R. Solé, *Integr. Biol.* **2016**, *8*, 485.
- [137] J. J. Velazquez, E. Su, P. Cahan, M. R. Ebrahimkhani, *Trends Biotechnol.* **2018**, *36*, 415.
- [138] A. Kicheva, N. C. Rivron, *Development* **2017**, *144*, 733.
- [139] M. K. Rice, W. C. Ruder, *Sci. Technol. Adv. Mater.* **2014**, *15*, 014401.
- [140] A. Y. Chen, Z. Deng, A. N. Billings, U. O. Seker, M. Y. Lu, R. J. Citorik, B. Zakeri, T. K. Lu, *Nat. Mater.* **2014**, *13*, 515.
- [141] J. E. Dueber, G. C. Wu, G. R. Malmirchegini, T. S. Moon, C. J. Petzold, A. V. Ullal, K. L. J. Prather, J. D. Keasling, *Nat. Biotechnol.* **2009**, *27*, 753.
- [142] L. Poshyvailo, E. von Lieres, S. Kondrat, *PLoS One* **2017**, *12*, e0172673.
- [143] A. Carvalho, D. B. Menendez, V. R. Senthivel, T. Zimmermann, L. Diambra, M. Isalan, *ACS Synth. Biol.* **2014**, *3*, 264.
- [144] R. Kwok, *Nature* **2010**, *463*, 288.
- [145] F. Ceroni, T. Ellis, *Nat. Rev. Mol. Cell Biol.* **2018**, *19*, 481.
- [146] B. Jusiak, S. Cleto, P. Perez-Pinera, T. K. Lu, *Trends Biotechnol.* **2016**, *34*, 535.
- [147] K. Kolar, W. Weber, *Curr. Opin. Biotechnol.* **2017**, *47*, 112.